Synergistic sorption/photo-Fenton removal of polycyclic aromatic hydrocarbons from coking wastewater over CuO-Montmorillonite

Ayman N. Saber[1, 2, 3,*], Ridha Djellabi[4,*], Claudia L Bianchi[4]

[1]National Engineering Laboratory for Industrial Wastewater Treatment, Research Center for Eco-Environmental Sciences, Chinese Academy of Sciences, Beijing, 100085, China

[2]University of Chinese Academy of Sciences, Beijing, 100049, China

[3]Pesticide Residues and Environmental Pollution Department, Central Agricultural Pesticide Laboratory, Agricultural Research Center, Dokki, Giza 12618, Egypt.

[4]Department of Chemistry, Università degli Studi di Milano, via Golgi 19, 20133, Milano, Italy

Corresponding authors: Ayman N. Saber (Ayman.nabil89@gmail.com); Ridha Djellabi (ridha.djellabi@yahoo.com)

Abstract

Polycyclic aromatic hydrocarbons (PAHs) and substituted PAHs (SPAHs) are common persistent organic pollutants that may be found in different industrial and agricultural wastewaters. In the present research study, we investigated the purification of coking wastewater containing mixed of 16 PAHs and 18 SPAHs compounds using CuO decorated Montmorillonite (CuO-M) under solar light. For better removal efficiency, H_2O_2 was added to make the photo-Fenton reaction into action. Due to the complexity of this coking wastewater, the purification was carried out in two runs. The results showed that, by using CuO-M/H_2O_2/light, 66% of the total yield of PAHs and SPAHs was removed from coking wastewater within 4 h. The second treatment run led to a further increase in the removal rate up to 91% of total pollution. Different synergetic mechanistic pathways such as the adsorb & shuttle process, generation of reactive oxygen species (ROSs) by photoactive CuO on the montmorillonite surface, and photo-Fenton ROSs generation in bulk water catalyzed by CuO and H_2O_2 are responsible for the effective removal of PAHs and SPAHs. Even though the study was established under well-controlled lab conditions, we should say that the CuO-M/H_2O_2/light system showed excellent performance in removing a significant part of PAH and SPAH compounds that might make it a potential alternative/cooperative to be involved in wastewater treatment plant (WWTP) to purify the same coking wastewater.

Keywords: Coking wastewater, Polycyclic aromatic hydrocarbons, CuO-Montmorillonite, Sorption, Photocatalysis, Photo-Fenton.

1. Introduction

Water pollution has long been considered as the leading risk factor for the environment and human health. In recent decades, due to the huge industrial activities, water pollution by different toxic stable compounds got out of control in many countries [1, 2]. In particular, coking wastewaters are polluted with high concentrations of harmful organic pollutants, including phenols, polycyclic aromatic hydrocarbons (PAHs), substituted PAHs (SPAHs), BTEX, etc. [3-5]. Since most of these chemicals are refractory, carcinogenic, and mutagenic, the pollution generated through coking wastewaters is a severe concern to the scientific and industrial community, particularly in developing countries. The existence of PAHs and SPAHs have gained great scientific interest due to them being among the most carcinogenic, mutagenic, and toxic pollutants in the environment [3, 6, 7].

Earlier studies demonstrated that coking wastewater contains significant quantities of high molecular weight (HMW) such as SPAHs and PAHs in the coking wastewater and sludge [3, 8]. PAHs and SPAHs are typically resistant to biological degradation and are ineffectively removed by traditional physio-chemical techniques such as flocculation, sedimentation, filtering, or ozonation [9, 10]. Adsorption and advanced oxidations are major approaches for reducing PAHs and SPAHs pollution in the environment, which have long been a hot topic in scientific studies [11-14]. Given its simple operations, non-existent secondary by-products, and the cost-effectiveness of investment and maintenance, the adsorption technique for aqueous PAHs and SPAHs pollution control is environmentally friendly and comparatively economic [15, 16]. Several studies have been reported on the treatment of coking wastewater by the use of different technologies such as electrochemical peroxidation process [17], adsorption combined with UV photocatalysis and electrochemical [18], photocatalysis over Ce-Ti-Graphene [19], photocatalysis-Fenton over a Fe-g-C_3N_4 graphene hydrogel 3D structure [20], photocatalysis-Fenton over Fe-doped g-C_3N_4 [21], photocatalysis-Fenton over rGH/Fe-g-

C_3N_4, TiO_2 photocatalytic synergized with ultrasonic [22], photocatalysis over reduced graphene oxide-polyaniline [23], combined photocatalytic-adsorption using n-Ce-TiO_2 and modified inferior coal char [24] and combined electrocoagulation with photo-Fenton [25]. As mentioned above, most recent studies have investigated the treatment of coking wastewater using combined systems due to the complexity of such wastewaters. Among them, photocatalysis has attracted a lot of attention from the scientific community. As an advanced oxidation process, photocatalysis has been used widely to oxidize stable organic pollutants via the photogenerated reactive oxygen species [26]. However, this green approach has recently received criticism due to many technology factors and misconducting of research studies, ignoring the photocatalytic tests in quasi-similar actual conditions [27, 28]. In fact, some studies have investigated the photocatalytic oxidation of mixed PAHs in water [29-31]. The main drawbacks of using naked photocatalytic nanoparticles are the low removal speed, generation of by-products due to the low adsorption ability, toxicity of nanoparticles in treated waters, and so on. Djellabi et al. [32] recently have critically discussed the significant strengths and weaknesses of photocatalytic technology. The authors reported that the scientific community has mostly addressed the removal of single pollutants, i.e., dyes, which are far from the real conditions. Further investigations to purify waters and wastewaters containing a high yield of multi-pollutants should be addressed to help transfer of this technology to real application [33].

Combining sorbing materials and photocatalytic nanoparticles on the same platform is fascinating to solve common issues found in a single process [34, 35]. The sorbing area can concentrate the pollutants near the photoactive area, allowing promoted surface oxidation reaction by the photogenerated reactive oxygen species (ROSs) through the so-called adsorb & shuttle process [36]. This process speeds up the overall removal and photooxidation processes and allows the continuous cleaning of the adsorbent surface. Several adsorbents

could be used alternatively to cost-effective commercial activated carbon, out of which clays have been proved to be very effective as adsorbents and also can amazingly immobilize photocatalytic nanoparticles, e.g., montmorillonite [34]. Bai et al. [37] reported that the combination of TiO_2 with graphene significantly enhances the removal of PAHs from water due to the synergistic effects between adsorption and photocatalysis.

As mentioned above, photocatalysis has recently received criticism because of its rare practice in the real world; the present research study is devoted to investigating a real case of coking wastewater purification, which was recovered from a wastewater treatment station (WWTP) after biological treatment. This wastewater is expected to be subjected to multi-stage advanced oxidation before discharging into the environment. The accurate evaluation of photocatalysis technology should be carried out compared to the existing technologies used for similar stages. Photocatalysis could be used during tertiary treatment in WWTP. CuO-montmorillonite based materials have been found to be effective for (photo)-catalytic or/and adsorption of different pollutants such as mercury [38, 39], lead [40], microorganisms [41-43], anthracene [39] dyes [44, 45], monocrotophos [46], sulfur mustard [47] and dichlorvos [48]. In the present study, the photocatalytic system in terms of CuO-montmorillonite/H_2O_2/solar light was used to treat coking wastewater which contains 34 mixed PAHs and SPAHs toxic compounds. Control experiments, including dark adsorption, photolysis, and photocatalysis were carried out separately to understand the mechanistic pathways.

2. Experimental section

2.1 Chemicals and sampling

The individual standards of 18 SPAHs, including 9 MPAHs, 5 NPAHs, and 4 OPAHs, were obtained from Tokyo Chemical Industry (TCI), American AccuStandard Company, Dr. Ehrenstorfer (Augsburg, Germany), and Toronto Research Chemicals Inc (TRC). At the same time, the 16 priority PAH chemicals were acquired from Ehrenstorfer (Augsburg, Germany).

The surrogate standard naphthalene-d8 was obtained from Dr. Ehrenstorfer (Augsburg, Germany).

Wastewater samples were taken from the biologically treated effluent of a coking wastewater treatment plant (WWTP) in northern China. This WWTP receives the discharge of the local coking factory, which indicates that the chemical composition of the biological effluent is quite complex. Wastewater samples were collected in glass containers, kept in the icebox, and then taken directly to the lab for analysis and treatment. The coking wastewater characterization was provided in our previous study [3].

2.2. Synthesis and characterization of CuO-Montmorillonite

The synthesis of CuO-Montmorillonite (CuO-M) was carried out by in situ precipitation of CuO on the surface of montmorillonite. Briefly, $CuSO_4 \cdot 5H_2O$ solution (1 M) was dropped on a water-montmorillonite mixture and stirring at 80◦C. Then, NaOH solution (1 M) was dropped, and the mixture was kept under stirring for 4 h. The obtained solid was washed several times by water in an ultrasonic bath. Finally, the solid was calcined at 200◦C for 2 h.

SEM image of bare montmorillonite was recorded on scanning electron microscopy (FEG LEO 1525, Zeiss Company, Germany). Thermogravimetry–differential thermal analysis (TG) on CuO-M from 25 to 500 °C was tested using thermogravimetric analyzer (NETZSCH STA 409 PC/PG). XRD spectrum of CuO-M was obtained using PANalytical X'PERT-PRO diffractometer with monochromatic CuKα radiation ($\lambda = 1.54056$ Å). Ultraviolet–visible light diffuse reflectance spectra (UV–VIS DRS) analysis of CuO-M was checked using Hitachi U-3900 Spectrophotometer equipped with an integrating sphere assembly ($BaSO_4$ salt was used as reference). Spectra of Fourier transform infrared spectroscopy analyses (FT-IR) on bare M and CuO-M were recorded on Nicolet iZ10 FT-IR Spectrometer (Thermo Fisher scientific).

2.3. Analytical methods

The initial evaluation of the biological effluent wastewater was determined by chemical oxygen demand (COD) and dissolved organic carbon (DOC) analysis. However, once the optimum conditions were established, the untreated (field sample) and treated wastewater samples were analyzed for determining PAHs and SPAHs concentration using headspace solid-phase microextraction (HS-SPME) as described by Saber et al., [3]. In brief, 10 mL of wastewater sample containing the surrogate at 0.5 $\mu g \cdot mL^{-1}$ was placed in an 18 mm vial with adding 2.6 g of sodium chloride. Then, the vials were sealed with a septum cap and pre-heated at 65°C (3 min); Afterward, a 75 µm carboxen/polydimethylsiloxane (CAR/PDMS) fiber was placed into the vial headspace, and the extraction was carried out at 65 ◦C for 25 min.

The target PAHs and SPAHs in the extracts were analyzed using a GC-MS Shimadzu QP2010 Plus (Kyoto, Japan) equipped with a Restek Rtx®-5Sil MS fused silica capillary column 30 m× 0.25 mm ID × 0.25 µm (film thickness) (Bellefonte, PA, USA). The SPME fiber (75 µm CAR/PDMS) was placed into the GC-MS injection port and desorbed at 290 °C for 10 min in splitless mode. The oven temperature program was as follows: 40◦C (5min); 10°C min^{-1} to 210 ◦C (1 min); 12 ◦C min^{-1} to 300 ◦C (10 min). The mass detector conditions for samples were: ion source temperature – 250 °C; MS interface line – 260°C; ionization mode– electron impact at 70 eV.

3. Results and discussion

Montmorillonite is a layer of structured clay with excellent porosity and external surface area. As discussed in our previous studies, it has a high cation exchange capacity and swelling property, facilitating its functionalization with metal oxides [34, 36]. Figure 1.a shows SEM image of bare montmorillonite that is used as a support for CuO oxide. The porous nature of this clay allows the successful support of CuO oxide. During the in-situ precipitation of CuO into the surface of Montmorillonite, Cu^{2+} can enter as a first step into the interlayer of the montmorillonite. When NaOH is added, CuO can be formed both on the external surface and

Commentato [CLB1]: rephrase

into the interlayers in the form of pillars. The BET surface area of montmorillonite is 49 m^2/g. Figure 1.b shows TG analysis of CuO-M, from 25 to 500°C, in which it can be observed two mass loss stages, one from 25 to ~195°C with mass change of 5.75% which is due to desorption of physically adsorbed water, and a small second mass change of 0.7% corresponding to removal of structural adsorbed water. This result shows the importance of montmorillonite clay as a support as it exhibits an excellent swelling behavior [36], which in turn enhances the generation of oxidative ROSs; the more the water molecules surrounded by the photocatalyst, the more ROSs photogeneration is obtained. Figure 1.c shows the XRD spectrum of CuO-M. The main characteristic diffraction peak of the montmorillonite crystal was detected at (2θ) = 20° [49]. A distinctive peak due to the presence of quartz was detected at (2θ) = 27°. Diffraction peaks showing the presence of monoclinic phase of CuO oxide on the surface of montmorillonite were detected at 2θ = 32° (1 1 1), 38° (−1 1 1), 48° (−2 0 2), 58.24° (2 0 2) and 62° (−1 1 3). As shown in Figure 1,d, the CuO-M spectrum shows a broadly visible light-responsive, allowing direct solar light to treat water in real conditions. Figures 1.e,f show FTIR spectra of bare M and CuO-M, respectively. The strong band at around 1000 cm^{-1} is due to Si-O stretching in-plane. Characteristic band of stretching vibration modes of OH groups with Al^{3+} is detected at 3600 cm^{-1}. The bands at around 3400 and 1600 cm^{-1} are due to the adsorbed water molecules. In CuO-M, the band at 3400 cm^{-1} became larger, probably due to OH groups coordinated to octahedral Cu^{2+} [50]. In addition, the peak at 3600 cm^{-1} was decreased in CuO-M, which might be due to the partial substitution of Al-OH by Cu-OH [43].

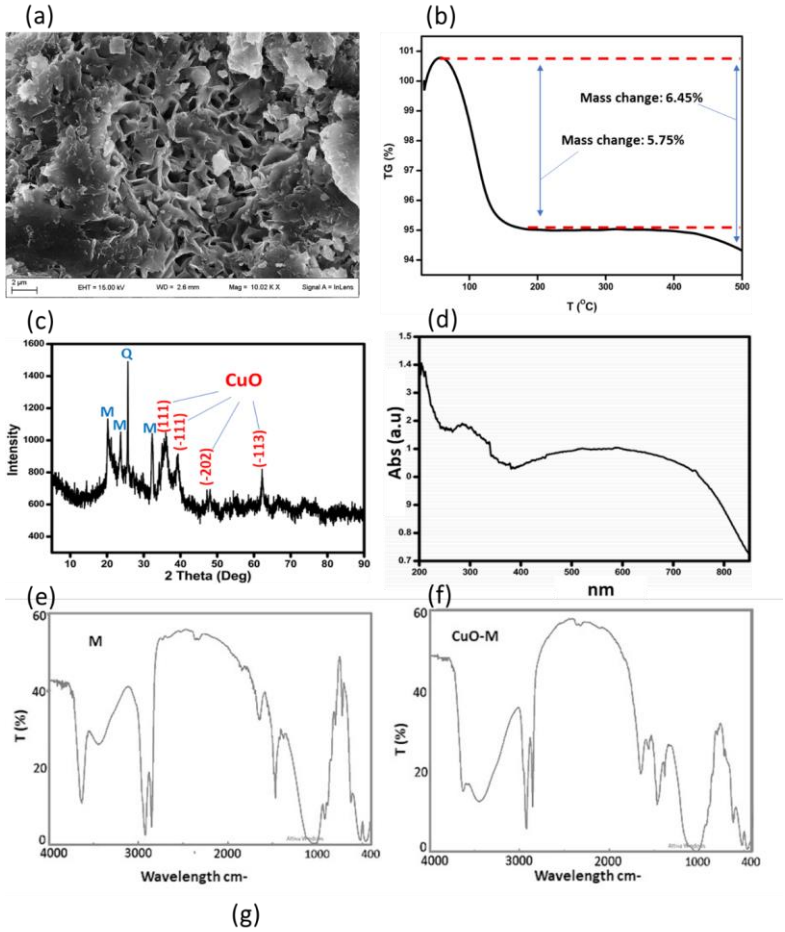

Figure 1. (a) SEM image of bare montmorillonite. (b): TG analysis of CuO-M sample. (c) XRD spectrum of CuO-M sample. (d) UVDRS spectrum of CuO-M sample. (e) and (f) FTIR spectra of bare montmorillonite and Cu-M samples, respectively.

The combined sorbing/photocatalytic ability of CuO-M was evaluated to treat very complicated real coking wastewater, which contains 34 toxic persistent organic compounds (PAHs and SPAHs). For the purpose of comparison, the purification of coking wastewater was carried out by different systems, including direct photolysis under solar light, dark adsorption by CuO-M, CuO-M/light, and CuO-M/light/H_2O_2. Since the first CuO-M/light/H_2O_2 could not

treat the wastewater ideally, a second run was performed using the CuO-M/light/H_2O_2 system on the obtained sample. The removal results by different methods are listed in **Table 1**. The main important task is to maximize the removal of PAHs and SPAHs yields from coking wastewater. The estimated total removal efficiency by the first and second treatments is shown in **Figure 2a**. It can be noticed that around 66% of total removal was obtained with the first treatment. The second treatment further enhanced the removal up to 91 %. During the first treatment, 8 compounds out of 34 were removed completely, while after the second treatment, only 6 compounds were detected in wastewater. We notice that the first treatment removed a high yield of compounds compared to the second treatment, and this is quite logical since the removal of nano-pollution is quite challenging because of the lower mass transfer.

Firstly, we should note that the combination of H_2O_2 and CuO-M under light has significantly promoted the removal of pollutants in all cases, compared to other systems. Although the concentration of compounds in coking wastewater is not the same, the photolysis, sorption, and photooxidation behaviors are entirely different depending on the pollutant type. Such diversity in terms of mechanistic removal by different systems depends on many factors, including the chemical structure and stability of each PHA/SPAH. The structure and charge of pollutant species can influence their fixation on CuO-M, which affects their oxidation by ROSs photogenerated on the surface of the photocatalyst. However, it is essential to point out that high competition appears among species in such a complex water matrix system to occupy the adsorptive sites and consume photogenerated ROSs.

To simplify the results, the removal process was classified into three categories: (i) pollutants removed by the first treatment, (ii): contaminants removed after the second treatment, and (iii): pollutants remain in wastewater even after the second treatment. Selected pollutants are shown in **Figures 2, b,c,d**, respectively. In general, it can be seen that the concentration of a single pollutant is not a key factor; some compounds with higher

concentration were removed effectively (such as Fluoranthene: 21μg/L), while others, at trace concentration, i.e., Acenaphythylene, were hard to remove and remain in the solution.

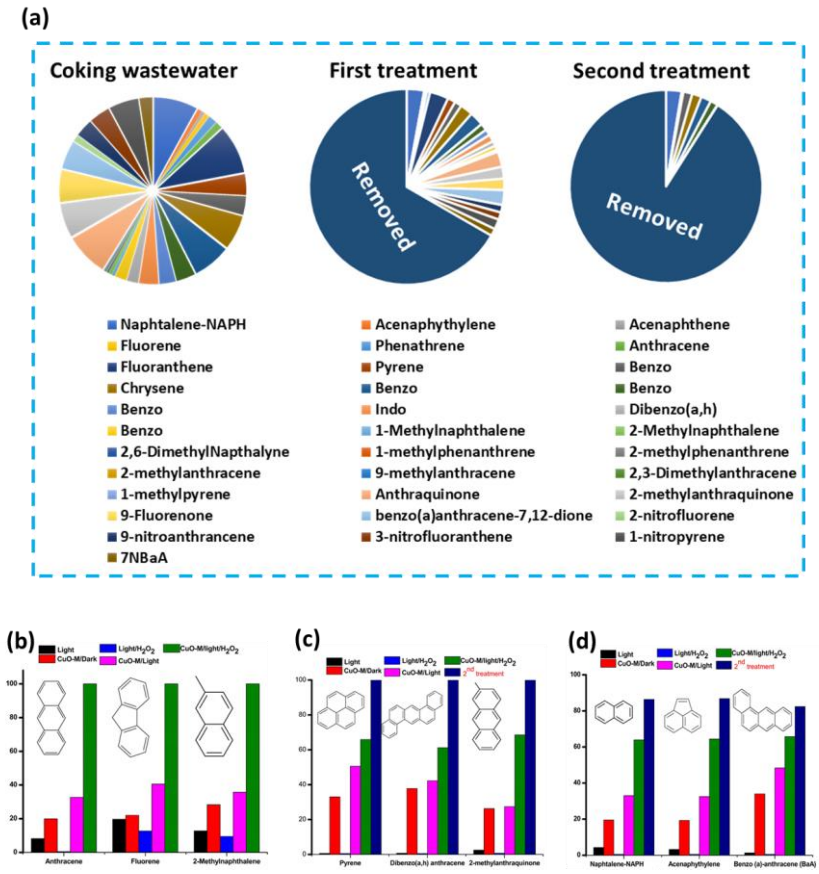

Figure 2. (a): Treatment of coking wastewater by M-CuO/H_2O_2 system under solar light within 4 h. The second treatment was carried on the treated wastewater by the first treatment. [CuO-M]: 1 g/L, [H_2O_2]: 10^{-3} M. Results of removal of selected organic pollutants by different systems within 4 h, (b): pollutants removed by the first treatment, (c): pollutants removed after the second treatment, (d): pollutants remain in the water after the second treatment.

Overall, the removal process using CuO-M/light/H_2O_2 showed great ability to treat such complex wastewater. It is essential to point out that the purification at large scale central WWTP of this wastewater is carried out by several successive purification steps, including adsorption, coagulation, and oxidation processes (chemical and Fenton). The reason behind such an excellent performance in terms of the CuO-M/light/H_2O_2 system is due to the combined and synergistic effects which CuO-M/light/H_2O_2 can provide, as shown in **Figure 3**. The so-called Adsorb & Suttle process taking place on the CuO-M surface speeds up the photocatalytic activity. After that, the photogenerated ROSs from CuO can oxidize the nearby adsorbed PAHs and SPAHs.

On the other hand, the photogenerated electrons on the CuO surface react with H_2O_2 to generate hydroxyl radicals. The generated •OH through photo-Fenton reaction can oxidize PAHs and SPAHs on the montmorillonite surface and/or in bulk solution. The sorpting ability of montmorillonite can also limit the generation of toxic products as most of them can remain on the surface. It was reported in previous studies that photocatalytic oxidation using naked photocatalysts leads to generate highly toxic by-products [51-53].

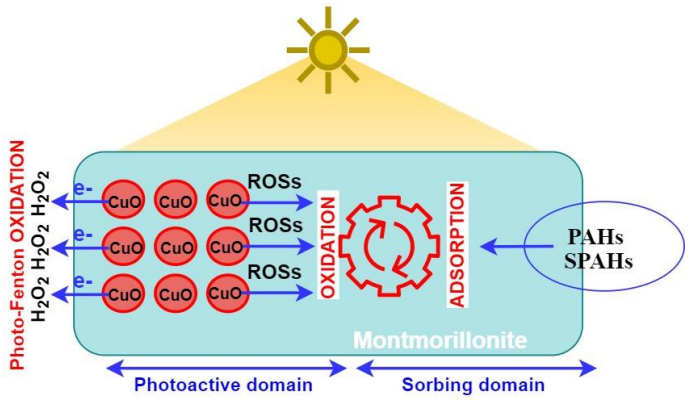

Figure 3. The photocatalytic mechanism on the surface of CuO-M in the presence of H_2O_2 under light irradiation towards the oxidation of PAHs and SPAHs in water.

259 **Table 1.** Results of the removal rates of 34 toxic organic compounds of mixed PAHs and

260 SPAHs from real coking wastewater by different systems

Compounds	Control, μg/L	Light	Adsorption	light/H_2O_2	M-CuO/light	M-CuO/light/H_2O_2	2st treatment
Naphtalene-NAPH	19.2	4.3	19.5	0.5	33.0	63.9	86.4
Acenaphythylene	2.1	3.2	19.3	0.5	32.5	64.4	86.8
Acenaphthene	1.2	2.3	27.6	1.5	31.9	64.4	100
Fluorene	2.3	19.7	22.0	12.7	40.6	100	100
Phenathrene	3.8	8.9	31.2	2.0	33.0	64.9	100
Anthracene	3.1	8.2	19.9	0.5	32.7	100	100
Fluoranthene	21.2	7.2	36.5	0.5	42.6	65.1	100
Pyrene	9.2	0.6	33.0	0.5	50.6	65.9	100
Benzo (a)-anthracene (BaA)	8.2	1.3	34.0	0.5	48.4	65.8	82.4
Chrysene	15.1	1.2	34.7	0.5	46.7	66.0	89.4
Benzo (B) Fluoranthene	16.6	1.3	35.2	0.5	44.4	66.2	89.7
Benzo (K) Fluoranthene	8.4	1.0	35.9	0.5	49.4	66.5	84.5
Benzo (a) Pyrene	7.1	0.9	36.5	0.5	50.7	66.7	100
Indo (1,2,3-cd) Pyrene	8.5	0.8	37.2	0.5	50.2	66.9	100
Dibenzo(a,h) anthracene	5.0	0.7	37.8	0.5	42.2	61.2	100
Benzo (g,h,i)Pyrlene	5.2	0.6	38.4	0.5	47.5	67.3	100
1-Methylnaphthalene	1.2	0.5	21.2	0.5	26.7	66.9	100
2-Methylnaphthalene	1.7	12.8	28.3	9.5	35.7	100	100
2,6-DimethylNapthalyne	0.5	3.1	28.7	0.5	29.8	61.8	100
1-methylphenanthrene	0.2	9.2	11.0	8.1	100	100	100
2-methylphenanthrene	0.2	1.1	37.5	13.2	41.6	71.6	100
2-methylanthracene	0.2	0.1	28.1	0.5	36.4	67.9	100
9-methylanthracene	0.4	0.5	100	100	100	100	100
2,3-Dimethylanthracene	0.3	5.4	25.7	0.5	100	100	100
1-methylpyrene	0.4	0.1	100	100	100	100	100
Anthraquinone	18.9	9.0	25.6	1.4	32.6	67.9	100
2-methylanthraquinone	14.9	2.5	26.3	0.7	27.4	68.5	100
9-Fluorenone	14.1	2.6	27.0	1.4	38.7	68.0	100
benzo(a)anthracene-7,12-dione	12.4	2.6	30.1	1.4	38.8	52.4	100
2-nitrofluorene	2.9	1.7	19.0	28.4	100	100	100
9-nitroanthrancene	7.8	5.5	19.1	1.0	33.8	62.1	100
3-nitrofluoranthene	9.2	0.9	31.1	0.9	47.9	68.3	100
1-nitropyrene	13.0	2.6	32.5	0.8	47.6	68.9	100
7NBaA	5.7	0.9	30.8	0.8	45.9	49.0	100

4. Conclusions

In the present study, we evaluate the efficiency of CuO-M/light/H_2O_2 to purify highly contaminated real coking wastewater by following all existing organic pollutants in terms of PAHs and SPAHs. The analysis of coking wastewater showed 34 toxic organic compounds of mixed PAHs and SPAHs with different concentrations. To properly understand the behavior of different PAHs and SPAHs during the treatment, coking wastewater was subjected to other treatment systems, including photolysis, adsorption, homogenous Fenton, photocatalysis over CuO-M, and combined Photo-Fenton-photocatalysis. It was noticed that each PAH or SPAH has different behavior in different systems, and it does not relate to the concentration of the pollutant species. Using CuO-M/light/H_2O_2, a total reduction in the yield of pollutants was recorded to be 66 % within 4h, while a second run on the same treated sample led to a removal rate of 91%. From the economic point of view, the results obtained in this study are encouraging because of the effective removal at low treatment cost. Several recent reports have successfully combined some technologies to purify coking wastewater properly; however, the same platform in terms of CuO-M/light/H2O2 may combine different mechanistic removal pathways, working cooperatively on the surface of the photocatalyst and the solution. We also emphasize identifying the organic composition before and after the treatment of coking wastewater by GC-MS, instead of simple characterization of such wastewaters by TOC, COD, and DOC due to the detection limits of these latter techniques. From technological, treating real cases of wastewater is by photocatalytic systems is very recommended to help to transfer this green technology to real-world application.

List of abbreviations:

M: Montmorillonite

CuO-M: CuO coated montmorillonite

PAHs: Polycyclic aromatic hydrocarbons

SPAHs: Substituted polycyclic aromatic hydrocarbons

ROSs: Reactive oxygen species

WWTP: Wastewater treatment plant

HMW: High molecular weight

COD: Chemical oxygen demand

DOC: Dissolved organic carbon

TOC: Total organic carbon

HS-SPME: Headspace solid-phase microextraction

CAR/PDMS: Carboxen/polydimethylsiloxane

XRD: X-ray powder diffraction

UVDRS: Ultraviolet–visible light diffuse reflectance spectra

SEM: Scanning electron microscopy

FTIR: Fourier transform infrared spectroscopy analysis

TG: Thermal gravimetric analysis

Acknowledgments

Dr Ayman N. Saber thanks the CAS-TWAS President's Fellowship's financial support for his Ph.D. study.

References

[1] P. Burmistrz, M. Burmistrz, Distribution of polycyclic aromatic hydrocarbons in coke plant wastewater, Water science and technology, 68 (2013) 2414-2420.
[2] X. Ma, X. Wang, Y. Liu, J. Gao, Y. Wang, Variations in toxicity of semi-coking wastewater treatment processes and their toxicity prediction, Ecotoxicology and Environmental Safety, 138 (2017) 163-169.
[3] A.N. Saber, H. Zhang, A. Islam, M. Yang, Occurrence, fates, and carcinogenic risks of substituted polycyclic aromatic hydrocarbons in two coking wastewater treatment systems, Science of The Total Environment, 789 (2021) 147808.
[4] A.N. Saber, H. Zhang, P. Cervantes-Aviles, A. Islam, Y. Gao, W. An, M. Yang, Emerging concerns of VOCs and SVOCs in coking wastewater treatment processes: Distribution profile, emission characteristics, and health risk assessment, Environmental Pollution, 265 (2020) 114960.
[5] A.N. Saber, H. Zhang, M. Yang, Optimization and validation of headspace solid-phase microextraction method coupled with gas chromatography–triple quadrupole tandem mass spectrometry for simultaneous determination of volatile and semi-volatile organic compounds in coking wastewater treatment plant, Environmental monitoring and assessment, 191 (2019) 1-17.

[6] S. Matsuzawa, L. Nasser-Ali, P. Garrigues, Photolytic behavior of polycyclic aromatic hydrocarbons in diesel particulate matter deposited on the ground, Environmental science & technology, 35 (2001) 3139-3143.
[7] M. Qiao, L. Fu, Z. Li, D. Liu, Y. Bai, X. Zhao, Distribution and ecological risk of substituted and parent polycyclic aromatic hydrocarbons in surface waters of the Bai, Chao, and Chaobai rivers in northern China, Environmental Pollution, 257 (2020) 113600.
[8] W. Zhang, C. Wei, X. Chai, J. He, Y. Cai, M. Ren, B. Yan, P. Peng, J. Fu, The behaviors and fate of polycyclic aromatic hydrocarbons (PAHs) in a coking wastewater treatment plant, Chemosphere, 88 (2012) 174-182.
[9] R. Crisafully, M.A.L. Milhome, R.M. Cavalcante, E.R. Silveira, D. De Keukeleire, R.F. Nascimento, Removal of some polycyclic aromatic hydrocarbons from petrochemical wastewater using low-cost adsorbents of natural origin, Bioresource technology, 99 (2008) 4515-4519.
[10] X. Liu, X. Yu, L. Sha, Y. Wang, Z. Zhou, S. Zhang, The preparation of black titanium oxide nanoarray via coking fluorinated wastewater and application on coking wastewater treatment, Chemosphere, 270 (2021) 128609.
[11] M. Boulangé, C. Lorgeoux, C. Biache, A. Saada, P. Faure, Fenton-like and potassium permanganate oxidations of PAH-contaminated soils: Impact of oxidant doses on PAH and polar PAC (polycyclic aromatic compound) behavior, Chemosphere, 224 (2019) 437-444.
[12] J. Chomanee, S. Tekasakul, P. Tekasakul, M. Furuuchi, Effect of irradiation energy and residence time on decomposition efficiency of polycyclic aromatic hydrocarbons (PAHs) from rubber wood combustion emission using soft X-rays, Chemosphere, 210 (2018) 417-423.
[13] W.-J. Dai, P. Wu, D. Liu, J. Hu, Y. Cao, T.-Z. Liu, C.P. Okoli, B. Wang, L. Li, Adsorption of polycyclic aromatic hydrocarbons from aqueous solution by organic montmorillonite sodium alginate nanocomposites, Chemosphere, 251 (2020) 126074.
[14] M. Davin, A. Starren, M. Deleu, G. Lognay, G. Colinet, M.-L. Fauconnier, Could saponins be used to enhance bioremediation of polycyclic aromatic hydrocarbons in aged-contaminated soils?, Chemosphere, 194 (2018) 414-421.
[15] S. Lamichhane, K.B. Krishna, R. Sarukkalige, Polycyclic aromatic hydrocarbons (PAHs) removal by sorption: a review, Chemosphere, 148 (2016) 336-353.
[16] M. Wang, S.E. Hearon, N.M. Johnson, T.D. Phillips, Development of broad-acting clays for the tight adsorption of benzo [a] pyrene and aldicarb, Applied clay science, 168 (2019) 196-202.
[17] F. Ozyonar, B. Karagozoglu, Treatment of pretreated coke wastewater by electrocoagulation and electrochemical peroxidation processes, Separation and Purification Technology, 150 (2015) 268-277.
[18] Q. Qin, H. Yang, H. Xu, J. Deng, R. Zhao, G. Huang, P. Wang, J. Wang, Experiment study on the separation of bituminous coal adsorption and the synergism of ultraviolet and electrochemistry in the pretreatment of coal chemical wastewater, Fuel, 288 (2021) 119712.
[19] J. Wen, Q. Zhang, G. Hu, Photocatalytic Degradation of Coking Wastewater by Ce-Ti-Graphene Composite, IOP Conference Series: Materials Science and Engineering, IOP Publishing, 2018, pp. 022021.
[20] J. Hu, P. Zhang, J. Cui, W. An, L. Liu, Y. Liang, Q. Yang, H. Yang, W. Cui, High-efficiency removal of phenol and coking wastewater via photocatalysis-Fenton synergy over a Fe-g-C3N4 graphene hydrogel 3D structure, Journal of Industrial and Engineering Chemistry, 84 (2020) 305-314.
[21] J. Hu, P. Zhang, W. An, L. Liu, Y. Liang, W. Cui, In-situ Fe-doped g-C3N4 heterogeneous catalyst via photocatalysis-Fenton reaction with enriched photocatalytic performance for removal of complex wastewater, Applied Catalysis B: Environmental, 245 (2019) 130-142.
[22] Z.-w. CHENG, D.-q. CANG, Research on Photocatalytic Treatment of Coking Wastewater Synergized with Ultrasonic [J], Journal of Wuhan University of Technology, 3 (2010).
[23] W. Cui, J. He, H. Wang, J. Hu, L. Liu, Y. Liang, Polyaniline hybridization promotes photo-electro-catalytic removal of organic contaminants over 3D network structure of rGH-PANI/TiO2 hydrogel, Applied Catalysis B: Environmental, 232 (2018) 232-245.

[24] J. Zhang, S. Wang, L. Liu, X. Zhang, B. Bi, D. Fu, Z. Li, Combined Treatment of Coking Wastewater with N-Ce-TiO2 and Modified Inferior Coal Char Combined Treatment of Coking Wastewater with N-Ce-TiO 2 and Modified Inferior Coal Char, Shanxi coal, 134 0.0932.
[25] M. Malakootian, M.R. Heidari, Removal of phenol from steel wastewater by combined electrocoagulation with photo-Fenton, Water Science and Technology, 78 (2018) 1260-1267.
[26] K. Bisaria, S. Sinha, R. Singh, H.M. Iqbal, Recent advances in structural modifications of photocatalysts for organic pollutants degradation–A comprehensive review, Chemosphere, (2021) 131263.
[27] M.G. Alalm, R. Djellabi, D. Meroni, C. Pirola, C.L. Bianchi, D.C. Boffito, Toward Scaling-Up Photocatalytic Process for Multiphase Environmental Applications, Catalysts, 11 (2021) 562.
[28] S.K. Loeb, P.J. Alvarez, J.A. Brame, E.L. Cates, W. Choi, J. Crittenden, D.D. Dionysiou, Q. Li, G. Li-Puma, X. Quan, The technology horizon for photocatalytic water treatment: sunrise or sunset?, ACS Publications, 2018.
[29] N. Vela, M. Martínez-Menchón, G. Navarro, G. Pérez-Lucas, S. Navarro, Removal of polycyclic aromatic hydrocarbons (PAHs) from groundwater by heterogeneous photocatalysis under natural sunlight, Journal of Photochemistry and Photobiology A: Chemistry, 232 (2012) 32-40.
[30] B. Liu, B. Chen, B.Y. Zhang, L. Jing, H. Zhang, K. Lee, Photocatalytic degradation of polycyclic aromatic hydrocarbons in offshore produced water: effects of water matrix, Journal of Environmental Engineering, 142 (2016) 04016054.
[31] V.-H. Nguyen, L.-A.P. Thi, Q. Van Le, P. Singh, P. Raizada, P. Kajitvichyanukul, Tailored photocatalysts and revealed reaction pathways for photodegradation of polycyclic aromatic hydrocarbons (PAHs) in water, soil and other sources, Chemosphere, 260 (2020) 127529.
[32] R. Djellabi, R. Giannantonio, E. Falletta, C.L. Bianchi, SWOT analysis of photocatalytic materials towards large scale environmental remediation, Current Opinion in Chemical Engineering, 33 (2021) 100696.
[33] J. Bi, Q. Tao, X. Huang, J. Wang, T. Wang, H. Hao, Simultaneous decontamination of multi-pollutants: A promising approach for water remediation, Chemosphere, (2021) 131270.
[34] R. Djellabi, M. Ghorab, G. Cerrato, S. Morandi, S. Gatto, V. Oldani, A. Di Michele, C.L. Bianchi, Photoactive TiO2–montmorillonite composite for degradation of organic dyes in water, Journal of Photochemistry and Photobiology A: Chemistry, 295 (2014) 57-63.
[35] Y. Zhu, T. Xu, D. Zhao, F. Li, W. Liu, B. Wang, B. An, Adsorption and solid-phase photocatalytic degradation of perfluorooctane sulfonate in water using gallium-doped carbon-modified titanate nanotubes, Chemical Engineering Journal, 421 (2021) 129676.
[36] R. Djellabi, M.F. Ghorab, A. Smara, C.L. Bianchi, G. Cerrato, X. Zhao, B. Yang, Titania–Montmorillonite for the photocatalytic removal of contaminants from water: adsorb & shuttle process, Green materials for wastewater treatment, Springer2020, pp. 291-319.
[37] H. Bai, J. Zhou, H. Zhang, G. Tang, Enhanced adsorbability and photocatalytic activity of TiO2-graphene composite for polycyclic aromatic hydrocarbons removal in aqueous phase, Colloids and Surfaces B: Biointerfaces, 150 (2017) 68-77.
[38] X. Zhang, L. Cui, Y. Li, Y. Zhao, Y. Dong, S. Cao, Adsorption and oxidation of mercury by montmorillonite powder modified with different copper compounds, Energy & Fuels, 33 (2019) 7852-7860.
[39] D.E. Egirani, M.T. Latif, N.R. Poyi, N. Wessey, S. Acharjee, SYNTHESIS AND CHARACTERIZATION OF CuO COATED MONTMORILLONITE AND ITS EFFECT ON MERCURY (II) IONS REMOVAL FROM AQUEOUS MEDIA, Journal of Chemical Technology & Metallurgy, 53 (2018).
[40] D.E. Egirani, N.R. Poyi, N. Wessey, Synthesis of a copper (II) oxide–montmorillonite composite for lead removal, International Journal of Minerals, Metallurgy, and Materials, 26 (2019) 803-810.
[41] A. Nouri, M.T. Yaraki, M. Ghorbanpour, S. Agarwal, V.K. Gupta, Enhanced Antibacterial effect of chitosan film using Montmorillonite/CuO nanocomposite, International journal of biological macromolecules, 109 (2018) 1219-1231.

[42] H. Pourabolghasem, M. Ghorbanpour, R. Shayegh, Antibacterial activity of copper-doped montmorillonite nanocomposites prepared by alkaline ion exchange method, Journal of Physical Science, 27 (2016) 1.
[43] S. Sohrabnezhad, M.M. Moghaddam, T. Salavatiyan, Synthesis and characterization of CuO–montmorillonite nanocomposite by thermal decomposition method and antibacterial activity of nanocomposite, Spectrochimica Acta Part A: Molecular and Biomolecular Spectroscopy, 125 (2014) 73-78.
[44] P. Tepmatee, P. Siriphannon, Nanoporous Copper Doped Aluminium Pillared Montmorillonite for Dye‐containing Wastewater Treatment, Water Environment Research, 88 (2016) 2015-2022.
[45] S. Sohrabnezhad, A. Pourahmad, T. Salavatiyan, CuO–MMT nanocomposite: effective photocatalyst for the discoloration of methylene blue in the absence of H 2 O 2, Applied physics A, 122 (2016) 1-12.
[46] K. Sahithya, D. Das, N. Das, Adsorptive removal of monocrotophos from aqueous solution using biopolymer modified montmorillonite–CuO composites: equilibrium, kinetic and thermodynamic studies, Process Safety and Environmental Protection, 99 (2016) 43-54.
[47] J.P. Kumar, P. Ramacharyulu, G. Prasad, B. Singh, Montmorillonites supported with metal oxide nanoparticles for decontamination of sulfur mustard, Applied Clay Science, 116 (2015) 263-272.
[48] K. Sahithya, D. Das, N. Das, Effective removal of dichlorvos from aqueous solution using biopolymer modified MMT–CuO composites: equilibrium, kinetic and thermodynamic studies, Journal of Molecular Liquids, 211 (2015) 821-830.
[49] A. Ahmed, Y. Chaker, E.H. Belarbi, O. Abbas, J. Chotard, H. Abassi, A.N. Van Nhien, M. El Hadri, S. Bresson, XRD and ATR/FTIR investigations of various montmorillonite clays modified by monocationic and dicationic imidazolium ionic liquids, Journal of Molecular Structure, 1173 (2018) 653-664.
[50] B. Tyagi, C.D. Chudasama, R.V. Jasra, Determination of structural modification in acid activated montmorillonite clay by FT-IR spectroscopy, Spectrochimica Acta Part A: Molecular and Biomolecular Spectroscopy, 64 (2006) 273-278.
[51] O. Woo, W. Chung, K. Wong, A.T. Chow, P. Wong, Photocatalytic oxidation of polycyclic aromatic hydrocarbons: intermediates identification and toxicity testing, Journal of Hazardous Materials, 168 (2009) 1192-1199.
[52] B. Liu, Enhanced photocatalytic oxidation of polycyclic aromatic hydrocarbons in offshore produced water, Memorial University of Newfoundland, 2018.
[53] J.J. Rueda-Marquez, I. Levchuk, P.F. Ibañez, M. Sillanpää, A critical review on application of photocatalysis for toxicity reduction of real wastewaters, Journal of Cleaner Production, 258 (2020) 120694.